Recharge Demand Mitigation for Latent Heat Thermal Energy Storage at Off-peak Hours

Al-Hussain OTHMAN[1], Vikrant AUTE[2]*, James TANCABEL[3]

[1,2,3]Center for Environmental Energy Engineering
Department of Mechanical Engineering, University of Maryland
College Park, MD 20742, USA
Email: [1]aothman@umd.edu, [2]vikrant@umd.edu, [3]jmtanc@umd.edu

* Corresponding Author

ABSTRACT

The utilization of integrated heat pump thermal energy storage (HP-TES) systems for space conditioning applications can reduce electrical power demand and achieve utility savings resulting from peak shaving and load shifting. However, issues arise when the energy required to recharge the TES exceeds the shifted energy demand, especially in extreme climates where high-temperature lifts between the outdoor air conditions and phase-change materials (PCMs) during recharing may occur. In this work, a single room-temperature (22°C) PCM-TES is integrated into a single-speed heat pump system using a secondary hydronic loop where the TES is recharged using the outdoor unit during off-peak hours. Three recharge strategies were investigated as potential pathways to reduce recharging power demand: (i) considering different heat source/sink temperatures, (ii) using a variable-speed compressor, and (iii) using a variable-speed pump. Simulations were conducted using Modelica for HP-TES recharging at different heat source/sink temperatures from -30 – 20°C in heating mode and 0 – 30°C in cooling mode. Results show that the most effective recharge demand reduction strategy is an HP-TES system using a single-speed compressor with a variable-speed pump for the hydronic loop run at preferable heat source/sink temperatures when the temperature lifts were reduced. Utilizing a variable-speed compressor for the HP-TES system reduced recharge time in extreme cases at the cost of additional compressor power input. The findings motivate potential control strategies that minimize recharge energy and maximize peak energy savings, hence reducing overall operating costs and annual energy consumption for HP-TES systems for space conditioning applications.

1. INTRODUCTION

In recent years, there has been an effort to electrify space conditioning (heating and cooling) in the US, resulting in 5% annual increases in space cooling energy consumption (IEA, 2021). With building space conditioning, water heating, and refrigeration representing around 50% of building energy consumption, there have been significant research efforts to utilize thermal energy storage (TES) with heat pumps (HPs) to curb growing strains on the electrical grid at peak hours (US Dept. of Energy, 2020). Current research efforts look into developing integrated systems, using ground-source heat pumps (Benli, 2011; Shi et al., 2021, 2022), air-source heat pumps (D'Ettorre et al., 2019; Ermel et al., 2023), and pre-cooling/heating air before entering the space conditioning heat exchangers (Chaiyat & Kiatsiriroat, 2014; Hai et al., 2022; Said & Hassan, 2018).

To assess the feasibility of HP-TES in the US, Sultan et al. (2023) conducted a techno-economic study looking at the suitable phase-change material (PCM) temperatures for different climate zones, using a rule-based-control strategy. The optimal PCM temperatures were 20°C and 30°C for cooling- and heating-dominated regions respectively. To maximize savings, HP-TES systems can reduce overall utility costs and annual energy consumption if optimal control strategies are applied. D'Ettorre et al., (2019) conducted sensitivity analyses for an HP combined with a sensible TES, utilizing model predictive controls on the system, looking at system challenges like lower outdoor temperatures, and heat loss from the TES. The authors found a maximum cost savings of 8%.

Nonetheless, the studies mentioned above do not highlight the challenges that come with recharging the TES system. Shi et al. (2022) simulated the TES system consisting of encapsulated phase-change materials and water combined with a ground-source heat pump and found that the required recharge time is at least twice the discharge time. However, their work does not discuss the implications of this issue in terms of the recharge energy demand or potential

impacts on the electrical grid. A subsequent study conducted shows that model predictive controls can be used to slightly lower the total annual energy for this system, and maintain indoor thermal comfort conditions, again without detailing the effect on the recharge energy and duration requirements (Shi et al., 2024). While HPs are considered the most efficient way to recharge TES (Li et al., 2020), it is important to consider all aspects of HP-TES operation during the recharge hours to ensure that both annual cost and energy savings are possible, without artificially creating another peak period during the recharge hours.

In this paper, we utilize transient Modelica simulations to analyze the increase in the recharge energy requirements of HP-TES at extreme climate conditions to compare the total recharge energy to the energy shifted during peak hours. Transient simulations in Modelica were utilized to investigate strategies that may reduce the required energy and time for TES recharge. Strategies include using variable-speed water pumps, and compressors, along with identifying the most suitable heat source and sink temperatures to discharge and recharge the TES. Using this analysis, recommendations can be made on how to operate the HP-TES to target cost and energy savings, ensuring that the recharge energy does not strain the grid, creating another peak period.

2. METHODOLOGY

2.1 System Description

The proposed HP-TES system consists of a 4-ton (14.1 kW) dual-purpose (heating and cooling) air-source R410A heat pump, where a TES system using a single room temperature PCM with a mid-point phase-change temperature of 22°C is integrated using a secondary hydronic loop which connects to the primary HP through a plate heat exchanger (Figure 1). The HP-TES system is designed to discharge for 2 hours during the utility peak targeted for all ASHRAE US climate zones 1 – 8, the hottest to the coldest zones where the system is applicable. When the TES is discharged, the TES interacts with the indoor coil, serving as the heat sink in cooling mode and the heat source in heating mode. During TES recharge, the operation is reversed such that the TES is the heat source in cooling mode (solidifying the PCM) and the heat sink in heating mode (melting the PCM) via the outdoor heat exchanger (HX).

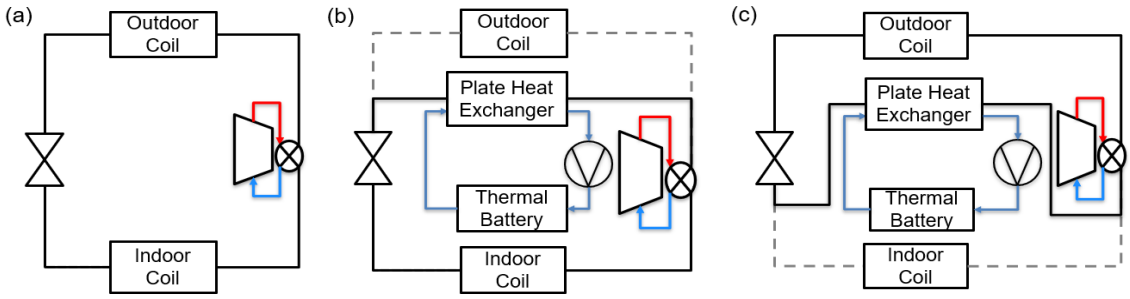

Figure 1: Dual-purpose operation for (a) baseline HP, (b) HP-TES discharge mode, (c) HP-TES recharge mode

2.2 HP-TES Modeling

The system was modeled using an in-house Modelica library (Qiao et al., 2015). The indoor and outdoor microchannel heat exchanger (MCHX) coils were modeled using three control volumes (CVs): (1) refrigerant CV, (2) wall CV, and (3) air-side CV. The model considers that the heat flow goes from the refrigerant CV, through the wall CV, to the air-side CV. The refrigerant CV solves the transient conservations of mass and energy equations. The two-phase refrigerant heat transfer coefficients were obtained from the Shah (2017) correlation for evaporation and Shah (2019) for condensation. The Dittus & Boelter, (1930) correlation was used to compute the single-phase refrigerant heat transfer coefficients. The air-side CV accounts for the total wall and fin surface areas, fin efficiency, and dehumidification rates, per tube, assuming that the wall and fin temperatures are uniform. More details about the MCHX can be found at Dhumane et al. (2021) and Qiao et al. (2015).

The baseline HP single-speed scroll compressor was modeled using a manufacturer-specified 10-coefficient compressor map and the Dabiri & Rice (1981) correction. Finally, the electronic expansion valve (Figure 2) was modeled using a variable orifice controlled using a PID controller from the Modelica Buildings Library (Wetter et al. 2014), and setting the superheat at 5 K.

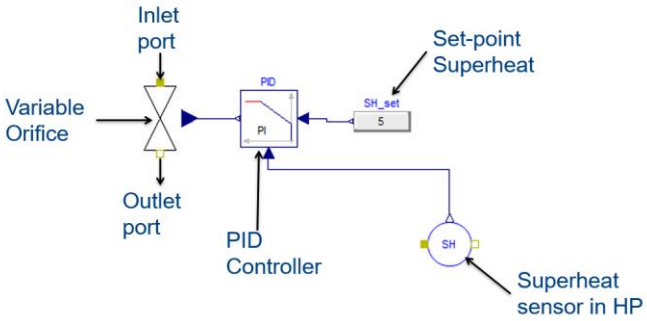

Figure 2: Electronic expansion valve model in Modelica

The hydronic secondary loop consists of (i) a single-speed water pump, (ii) the water-to-refrigerant PHX, and (iii) the thermal battery. The single-speed water pump power was calculated assuming a pump efficiency of 70%, and a fixed water mass flow rate was used to ensure that the water temperature change was 5 K (Equation (1)).

$$\dot{W}_{pump} = \frac{\dot{m}\Delta P}{\rho \eta} \tag{1}$$

Figure 3 shows how the PHX and thermal battery were represented in Modelica. The PHX model lumped all the channels and plates into the refrigerant control volume used in the MCHXs and a water control volume (Figure 3(a)). The correlations used for the refrigerant-side heat transfer coefficient correlations were Focke et al. (1985) for single-phase refrigerant and Yan et al., (1999) for two-phase refrigerant. The waterside CV heat transfer rate is calculated using Equation (2).

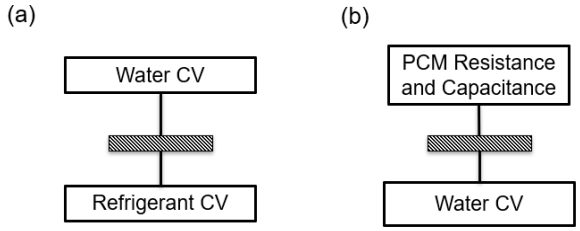

Figure 3: Representation of (a) PHX and (b) thermal battery in Modelica

$$\dot{Q}_{total} = \sum_{i=1}^{i=N_{seg}} h_{seg,i} A_{seg,i} (T_{wall,i} - T_{water,i-1}) \tag{2}$$

The thermal battery (Figure 3(b), utilizes the same water CV used in the PHX. In this case, the thermal battery uses 9.5-mm outer diameter tube-fin HX, where the heat transfer coefficient was determined using the Dittus & Boelter, (1930) correlation. The PCM side was modeled using a resistance-capacitance approach (Cao & Faghri, 1990; Dhumane et al., 2019). The resistance component of the model contains the heat transfer side of the model shown in Equation (3), where k is the PCM thermal conductivity, and L is the half distance between adjacent HX tubes.

$$\dot{Q}_{PCM} = \frac{k}{L} \sum_{j=1}^{j=N_{seg}} A_{seg,j} (T_{wall,j} - T_{water,j-1}) \qquad L = \frac{\sqrt{(VS - OD)^2 + (HS - OD)^2}}{2} \tag{3}$$

The capacitance (energy storage) side utilizes PCM-specific DSC curves to compute enthalpy as a function of PCM temperature; separate curve fits were made for melting and solidification. Once the enthalpy is calculated, the PCM discharge rate can be computed based on the change of enthalpy with respect to time (Equation (4)).

$$\dot{Q} = \sum_{j=1}^{j=N_{seg}} \frac{di_{PCM,j}}{dt} M_{PCM,j} \tag{4}$$

The capacitance and resistance components are connected using a `HeatPort` component from the `Modelica Standard Library` (2013).

2.3 Load-Shifting Scenarios and Impacts

Before addressing recharge mitigation strategies, it is important to understand the different load-shifting scenarios. The first step is to calculate the required energy for the baseline HP, the HP-TES discharge, the recharge energy, and the energy saved during the peak as per Equations (5) and (6), where the baseline unit energy is computed considering the compressor power with the indoor and outdoor fans. In some heating mode cases, backup heating energy (COP = 1) must be considered at low outdoor temperature applications when the HP cannot meet the rated 4-ton (14.1 kW) capacity. In discharge (recharge) mode, the outdoor (indoor) fan is disconnected and replaced with pump power from the secondary loop. The energy saved is the difference between the energy input for the baseline HP and HP-TES (discharging) during the peak.

$$E_{baseline,peak} = \int_{t=t_0}^{t=t_f} (\dot{W}_{comp} + \dot{W}_{fan,out} + \dot{W}_{fan,in} + \dot{W}_{backup})dt; \quad \dot{W}_{backup} = \dot{Q}_{rated} - \dot{Q}_{baseline} \tag{5}$$

$$\begin{aligned} E_{discharge} &= \int_{t=t_0}^{t=t_f} (\dot{W}_{comp} + \dot{W}_{fan,in} + \dot{W}_{pump})dt \\ E_{recharge} &= \int_{t=t_0}^{t=t_f} (\dot{W}_{comp} + \dot{W}_{fan,out} + \dot{W}_{pump})dt \\ E_{saved,peak} &= E_{baseline,peak} - E_{discharge} \end{aligned} \tag{6}$$

There are several potential load-shifting scenarios (Table 1). Ideally, the recharge energy should be lower than the peak energy saved. However, most of the time this is not the case, as the peak energy savings and recharge energy are highly dependent on the outdoor temperature and indoor loads. Cost savings are achievable if the recharge energy is below the baseline energy, but may strain the grid if it is above the discharge energy. Thus, it is important to ensure that the recharge energy is below the discharge energy.

Table 1: Scenarios matrix for recharge energy consumption when using HP-TES and load shifting

Recharge Energy Consumption	Energy Savings	Cost Savings	Comments	Strain on Grid
$E_{recharge} \le E_{saved,peak}$	✓	✓	Ideal	None / Minimal
$E_{saved,peak} \le E_{recharge} \le E_{discharge}$	✗	✓	Recommended	None / Minimal
$E_{discharge} \le E_{recharge} < E_{baseline}$	✗	✓	Re-design	Moderate
$E_{recharge} \ge E_{baseline,peak}$	✗	✗	Re-design	High

2.4 Recharge Energy Mitigation Strategies

2.4.1 Variable-speed water pump: The single-speed water pump is replaced with a variable-speed pump. In Modelica, the variable-speed pump was controlled by a PID from the Modelica Buildings Library (Wetter et al., 2014), altering the water flow rate to maintain a recharge rate of 4 tons (14.1 kW), reducing recharge required time. Pump affinity laws were used to compute the pumping power.

2.4.2 Variable-speed compressor: The single-speed compressor is replaced. The variable-speed compressor, represented by 20-coefficient maps, was controlled to maintain a consistent recharge rate at the rated unit capacity of 4 tons (14.1 kW), using the PID in Modelica (Wetter et al., 2014). The component modifications, pump, and compressor, were run solely and simultaneously, as shown in Table 2.

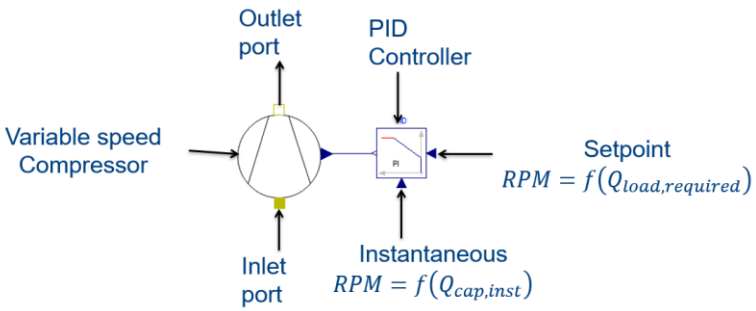

Figure 4: Variable-speed compressor model and controls in Modelica

Table 2 summarizes the components considered. When simulating the HP and HP-TES in discharge mode, the pre-coil temperature for the indoor HX was assumed to be 21.1°C (70°F) in heating mode, and 26.7°C (80°F) in cooling mode as per the AHRI Standard 210/240 (2023) H1 and A test conditions.

Table 2: HP-TES cycle components considered for the refrigerant cycle and hydronic loop

HP-TES Cycle	Compressor Type	Pump Type
1	Single-speed	Single-speed
2	Single-speed	Variable-speed
3	Variable-speed	Single-speed
4	Variable-speed	Variable-speed

2.4.3 Influence of heat source/sink temperature: The recharge energy required is primarily affected by the temperature lifts in the cycle. Consequently, finding the most suitable outdoor temperatures whether recharging for cooling or heating can significantly reduce the recharge energy required. Nighttime TMY3 temperatures in the US can range between 0 – 20°C in hot climate zones (e.g., 1A) or from -30 – 15°C in cold climate zones (e.g., 7). Additionally, indoor room temperatures in heating and cooling can typically be between 15 – 25°C Thus, the recharge energy was investigated for cooling mode when outdoor temperatures were between 0 – 25°C, and from -30 – 20°C in heating mode.

3. RESULTS AND DISCUSSION

3.1 Heating Mode

Evaluating the peak energy consumption (Figure 5), at lower ambient temperatures, the energy saved is higher as the HP-TES systems can meet the rated capacity of 4-tons (14.1 kW) without any backup heating of COP = 1. The warmer days do not require any backup heating. Replacing the single-speed with a variable-speed pump has minimal effects as the higher thermal resistances on the PCM side. The variable-speed compressor requires lower energy consumption in colder climate conditions, compressor speed increases to meet the rated conditions at a lower backup heating penalty. During warmer days, the compressor can work at a lower speed, thus operating at a higher efficiency to meet the system capacity, whereas the single-speed compressor would have to cycle on/off depending on the required load. Consequently, the energy savings when integrating the single-speed compressor with TES is higher, given the sudden drop in temperature lifts, increasing systems performance.

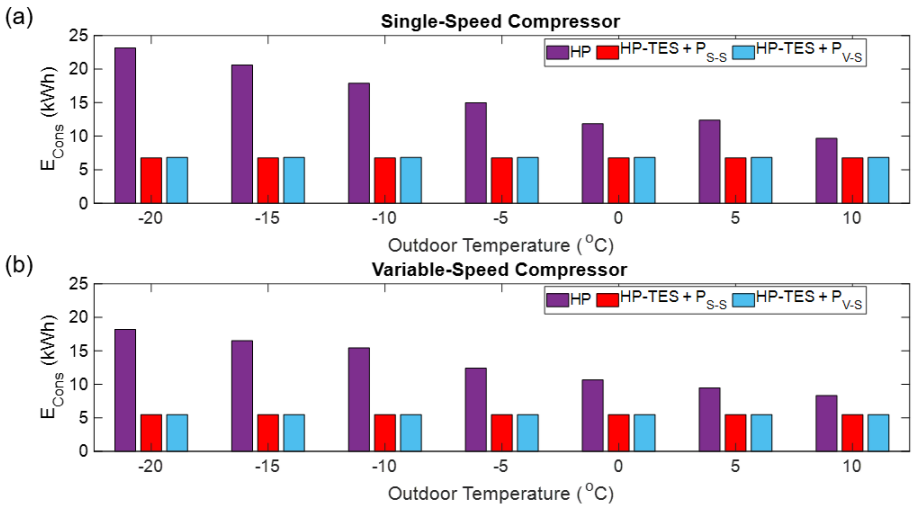

Figure 5: Peak energy required for the baseline HP, HP-TES + P_{S-S}, and HP-TES + P_{V-S} (a) single-speed compressor, and (b) variable-speed compressor

For all HP-TES cycles, increasing the heat source outdoor temperature significantly reduces the recharge time, given reduced temperature lifts and higher recharge rates (Figure 6). The variable-speed compressor systems have a 40% shorter recharge period at the extremes, operating at maximum speed and thus enabling a higher recharge rate. For warmer source temperatures, the single-speed compressors are faster, as they are not controlled to provide a specific recharge rate. The variable speed pump was only effective at warmer heat sink temperatures, as the PHX can get more heat from the system due to the increased water flow rate.

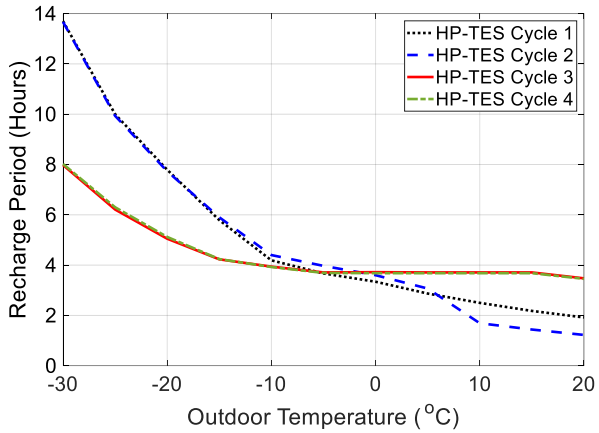

Figure 6: Required recharge time of the four HP-TES cycle components

When mapping the energy requirements, the single-speed compressor systems (Figure 7(a)) can have significant energy savings when recharge occurs at outdoor temperatures of 5°C or larger due to better balancing of recharge and discharge energy. However, this can only happen if TES discharge occurs during lower outdoor ambient temperature periods while it recharges at warmer ones. The results here show that regardless of components, decreasing the temperature lift during recharge is key to reducing the recharge energy. The influence of the variable speed pump was observed at outdoor air temperatures between 15 – 20°C, as the heat transfer between the PHX and the thermal battery increased given the higher water velocity, at lower temperature lifts.

The impact of the variable-speed compressor in reducing the recharge energy was minimal, around 8%, at a heat source temperature of -30°C. Furthermore, the variable-speed compressor systems limited the load-shifting potential as it reduced the baseline energy consumption compared to single-speed compressor systems. Thus, the variable-speed HP-TES cycle can significantly limit the useful operation of the TES to discharge at outdoor temperatures below -8°C if the TES is recharged at heat source temperatures between 15 – 20°C. This is the only way the HP-TES operation

will consume less energy than the baseline variable-speed energy. If the end-user is only looking for cost savings, then the recharge must occur at source temperatures 15 – 20 K higher than during peak hours, when the recharge energy is below the baseline energy. Thus, the most appropriate recharge hours are probably during noon as they might be the warmest hours, as peak utility hours in the winter are either the early morning hours or late afternoon hours.

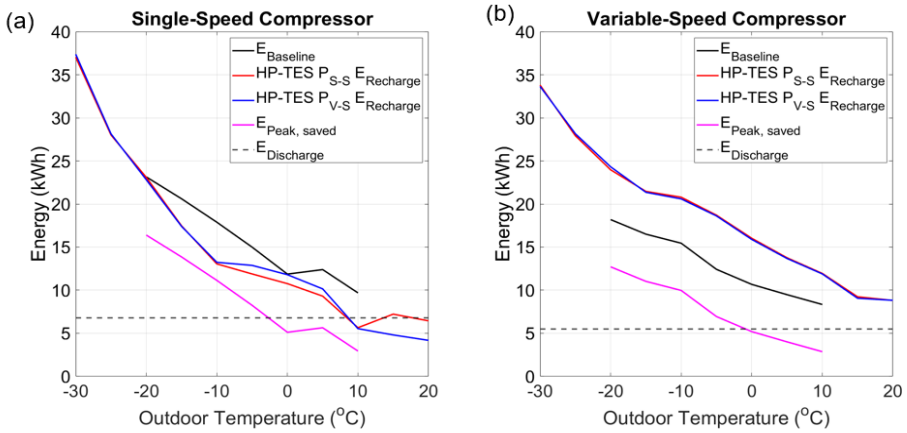

Figure 7: Heating mode recharge energy comparison: (a) single-speed compressor (b) variable-speed compressor.

3.2 Cooling Mode

The highest energy demand reduction from HP to HP-TES occurs at higher outdoor temperatures, given the temperature lift reductions (Figure 8). Temperature lifts affect both single and variable-speed compressors differently. At higher outdoor temperatures, the variable-speed compressor has a higher demand reduction as the compressor speed increases to meet the rated capacity of 4 tons (14.1 kW). Thus, reducing temperature lift when using a variable speed compressor has two advantages: (a) the compressor speed drops, reducing power demand, and (b) the compressor efficiency increases at lower compressor speeds, given lower entropy generation.

For the cooling case (Figure 9), the total recharge time was 2 – 3 hours for all the cycles when the outdoor temperatures were above 10°C. The lowest recharge time was 1.9 hours (1 hour and 54 minutes) for HP-TES cycle 2 (single-speed compressor, $P_{V\text{-}S}$) at 0°C, corresponding to nighttime temperatures during the shoulder season. At lower outdoor temperatures, the COP of the cycle increases, as the compressor efficiency and condenser heat transfer rate increase, speeding up the recharge rate. The highest recharge time was 3.5 hours for the complete single-speed system at 30°C. The systems using the variable speed compressors stabilized the recharge time at an average of 3.1 hours, as the compressor speed was modulated to recharge at a constant rate of 14 kW.

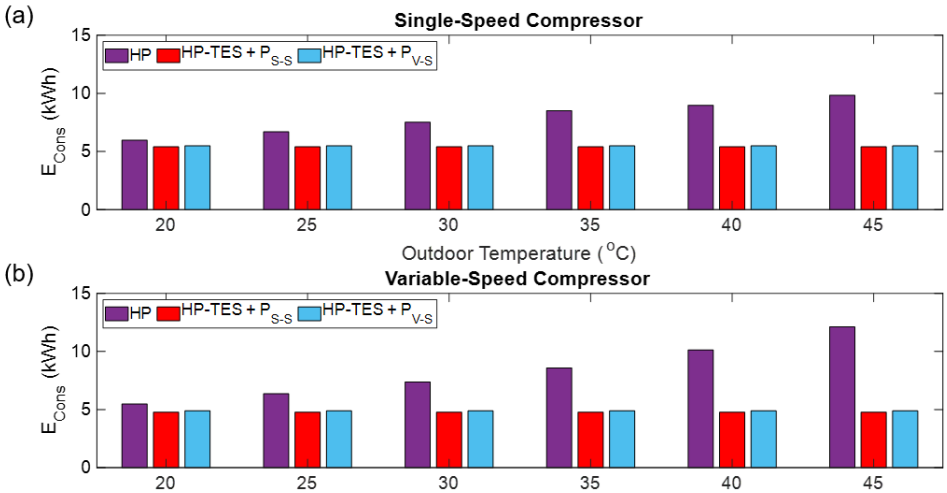

Figure 8: Peak energy required for the baseline HP, HP-TES + $P_{S\text{-}S}$, and HP-TES + $P_{V\text{-}S}$ (a) single-speed compressor, and (b) variable-speed compressor

To achieve energy savings, the recharge and discharge energy must be lower than the baseline energy during the peak hours (Figure 10). This can only happen when the outdoor temperatures during peak hours are greater than 40°C, and when the recharge hours heat sink temperatures are below 5°C. This may limit the potential useful locations for the HP-TES system if the primary objective is to save energy. Thus, maximizing cost savings by using a variable speed pump and limiting recharge energy is achievable by discharging the HP-TES when the outdoor temperature is above 30°C and recharging at temperatures below 15°C. An alternative solution would be to load shift as much energy as possible during the peak hours while ensuring the shifted energy is no more than that which can be recharged.

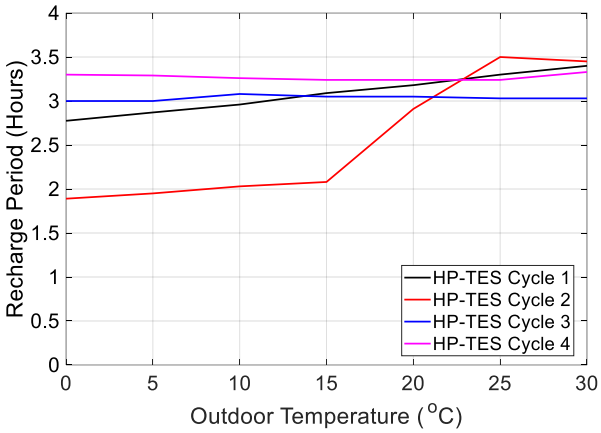

Figure 9: Required recharge time of the four HP-TES cycle components in cooling mode

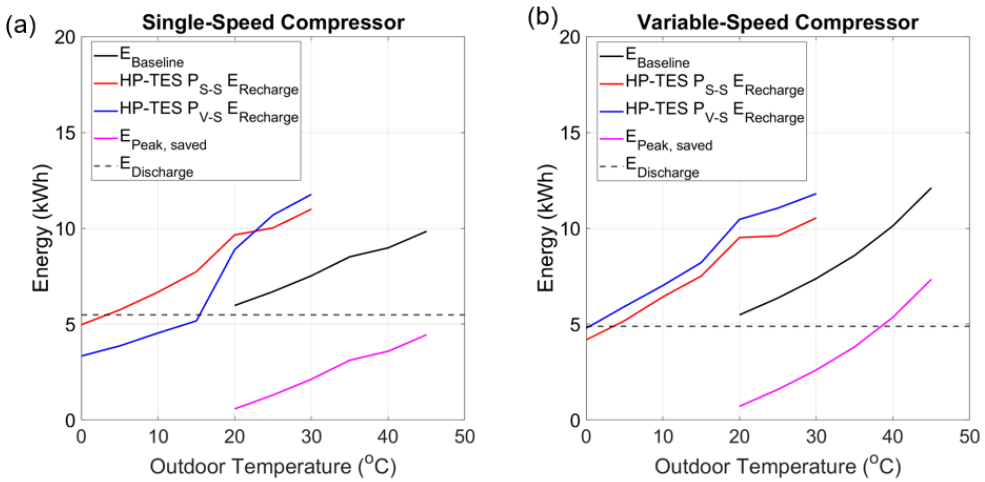

Figure 10: Cooling mode recharge energy comparison: (a) single-speed compressor; (b) variable-speed compressor.

4. CONCLUSIONS

This paper presents an analysis of mitigation strategies to reduce off-peak recharge energy for a dual-purpose HP-TES. These strategies include component changes, i.e., swapping single-speed pumps/compressors for variable-speed versions, and recharging at different heat source/sink temperatures. Transient models for the HP and HP-TES were created in Modelica, and the corresponding energy consumption and savings during discharge and recharge were compared. It was found that the most promising HP-TES system for recharge energy mitigation was equipped with a single-speed compressor and a variable-speed pump in both cooling and heating modes. Nonetheless, the main driver for reducing energy demand in recharge and discharge modes is reducing the temperature lifts. This corresponds to recharge at outdoor temperatures below 15°C in cooling mode and above 10°C in heating mode, and discharge at temperature above 30°C in cooling mode, or less than -5°C in heating mode. Variable-speed compressor HP-TES may not be suitable as recharge energy demand increases due to higher compressor speeds and longer recharge periods. The findings from these simulations can be used to develop a control strategy whose primary focus is to maximize the

peak energy savings, ensuring that the recharge energy requirements do not create another artificial peak period straining the grid at other hours of the day.

NOMENCLATURE

A	Area	(m^2)	P	Pump	(–)
COP	Coefficient of performance	(–)	$\dot{Q}$	Heat transfer	(kW)
E	Energy	(kWh)	T	Temperature	(°C)
h	Heat transfer coefficient	($W/m^2 K$)	t	Time	(s)
HS	Horizontal spacing	(m)	VS	Vertical spacing	(m)
i	Enthalpy	(kJ/kg)	$\dot{W}$	Power	(kW)
k	Thermal conductivity	(W/m K)	ΔP	Pressure drop	(Pa)
L	Length	(m)	η	Pump efficiency	(–)
M	Mass	(kg)	ρ	Density	(kg/m^3)
$\dot{m}$	Mass flow rate	(kg/s)			

Subscript

Exp	Expansion Valve	S-S	Single-speed
Seg	Segment	V-S	Variable-speed

REFERENCES

AHRI Standard 210/240. (2017). *Standard for Perforamnce Rating of Unitary Air-Conditioing and Air-Source Heat Pump*.

Benli, H. (2011). Energetic performance analysis of a ground-source heat pump system with latent heat storage for a greenhouse heating. *Energy Conversion and Management*, *52*(1), 581–589. https://doi.org/10.1016/j.enconman.2010.07.033

Cao, Y., & Faghri, A. (1990). A Numerical Analysis of Phase-Change Problems Including Natural Convection. *Journal of Heat Transfer*, *112*(3), 812–816. https://doi.org/10.1115/1.2910466

Chaiyat, N., & Kiatsiriroat, T. (2014). Energy reduction of building air-conditioner with phase change material in Thailand. *Case Studies in Thermal Engineering*, *4*, 175–186. https://doi.org/10.1016/j.csite.2014.09.006

Dabiri, A. E., & Rice, C. K. (1981). *Compressor-simulation model with corrections for the level of suction gas superheat* (CONF-810657-2). Oak Ridge National Lab., TN (USA); Science Applications, Inc., La Jolla, CA (USA). https://www.osti.gov/biblio/6345140

D'Ettorre, F., Conti, P., Schito, E., & Testi, D. (2019). Model predictive control of a hybrid heat pump system and impact of the prediction horizon on cost-saving potential and optimal storage capacity. *Applied Thermal Engineering*, *148*, 524–535. https://doi.org/10.1016/j.applthermaleng.2018.11.063

Dhumane, R., Ling, J., Aute, V., & Radermacher, R. (2021). Performance comparison of low GWP refrigerants for a miniature vapor compression system integrated with enhanced phase change material. *Applied Thermal Engineering*, *182*, 116160. https://doi.org/10.1016/j.applthermaleng.2020.116160

Dhumane, R., Qiao, Y., Ling, J., Muehlbauer, J., Aute, V., Hwang, Y., & Radermacher, R. (2019). Improving system performance of a personal conditioning system integrated with thermal storage. *Applied Thermal Engineering*, *147*, 40–51. https://doi.org/10.1016/j.applthermaleng.2018.10.004

Dittus, F. W., & Boelter, L. M. K. (1930). Heat transfer in automobile radiators of the tubular type. *University of California Publications in Engineering*,. https://doi.org/10.1016/0735-1933(85)90003-X

Ermel, C., Bianchi, M. V. A., & Schneider, P. S. (2023). Energy Model to Evaluate Thermal Energy Storage Integrated with Air Source Heat Pumps: Preprint. *Renewable Energy*.

Focke, W. W., Zachariades, J., & Olivier, I. (1985). The effect of the corrugation inclination angle on the thermohydraulic performance of plate heat exchangers. *International Journal of Heat and Mass Transfer*, *28*(8), 1469–1479. https://doi.org/10.1016/0017-9310(85)90249-2

Hai, T., El-Shafay, A. S., Zain, J. M., El-Rahman, M. A., & Sharifpur, M. (2022). The effect of triangular phase change material rods in the air conditioning duct on the amount of energy required for a residential building. *Journal of Building Engineering*, *52*, 104330. https://doi.org/10.1016/j.jobe.2022.104330

IEA. (2021). *Cooling*. IEA. https://www.iea.org/energy-system/buildings/space-cooling

Li, Y., Zhang, N., & Ding, Z. (2020). Investigation on the energy performance of using air-source heat pump to charge PCM storage tank. *Journal of Energy Storage*, *28*, 101270. https://doi.org/10.1016/j.est.2020.101270

Modelica/ModelicaStandardLibrary. (2024). [Modelica]. Modelica Association. https://github.com/modelica/ModelicaStandardLibrary (Original work published 2013)

Qiao, H., Aute, V., & Radermacher, R. (2015). Transient modeling of a flash tank vapor injection heat pump system – Part I: Model development. *International Journal of Refrigeration*, *49*, 169–182. https://doi.org/10.1016/j.ijrefrig.2014.06.019

Said, M. A., & Hassan, H. (2018). Parametric study on the effect of using cold thermal storage energy of phase change material on the performance of air-conditioning unit. *Applied Energy*, *230*, 1380–1402. https://doi.org/10.1016/j.apenergy.2018.09.048

Shah, M. M. (2017). Unified correlation for heat transfer during boiling in plain mini/micro and conventional channels. *International Journal of Refrigeration*, *74*, 606–626. https://doi.org/10.1016/j.ijrefrig.2016.11.023

Shah, M. M. (2019). Improved correlation for heat transfer during condensation in conventional and mini/micro channels. *International Journal of Refrigeration*, *98*, 222–237. https://doi.org/10.1016/j.ijrefrig.2018.07.037

Shi, L., Liu, X., Qu, M., Liu, G., & Li, Z. (2021). Potential of Utilizing Thermal Energy Storage Integrated Ground Source Heat Pump System to Reshape Electricity Demand in the United States. *ASME Journal of Engineering for Sustainable Buildings and Cities*, *2*(031003). https://doi.org/10.1115/1.4051992

Shi, L., Qu, M., Liu, X., Cui, B., & Dong, J. (2024). Performance Evaluation of a Model Predictive Control for Thermal Energy Storage Integrated Heat Pump Systems through a Co-Simulation. *ASHRAE Transactions*, *130*(Part 1).

Shi, L., Qu, M., Liu, X., Wang, L., & Zhang, M. (2022). Numerical modeling and parametric study of a dual purpose underground thermal battery. *Energy and Buildings*, *275*, 112472. https://doi.org/10.1016/j.enbuild.2022.112472

Sultan, S., Hirschey, J., Kumar, N., Cui, B., Liu, X., LaClair, T. J., & Gluesenkamp, K. R. (2023). Techno-Economic Assessment of Residential Heat Pump Integrated with Thermal Energy Storage. *Energies*, *16*(10), Article 10. https://doi.org/10.3390/en16104087

US Dept. of Energy. (2020). Thermal Energy Storage. *Energy.Gov*. https://www.energy.gov/eere/buildings/thermal-energy-storage

Wetter, M., Zuo, W., Nouidui, T. S., & Pang, X. (2014). Modelica Buildings library. *Journal of Building Performance Simulation*, *7*(4), 253–270. https://doi.org/10.1080/19401493.2013.765506

Yan, Y.-Y., Lio, H.-C., & Lin, T.-F. (1999). Condensation heat transfer and pressure drop of refrigerant R-134a in a plate heat exchanger. *International Journal of Heat and Mass Transfer*, *42*(6), 993–1006. https://doi.org/10.1016/S0017-9310(98)00217-8

ACKNOWLEDGEMENT

This material is based upon work supported by the U.S. Department of Energy's Office of Energy Efficiency and Renewable Energy (EERE) under the Building Technologies Office (BTO) Award Number DE-EE0009681. The views expressed herein do not necessarily represent the views of the U.S. Department of Energy or the United States Government. This work was also supported in part by the Modeling & Optimization Consortium at the Center for Environmental Energy Engineering at the University of Maryland.